The Role of Intermediate Phases in the Crystallization of Aluminophosphate Sieves on Examples of AlPO-11 and AlPO-41

Marat R. Agliullin [1],*, Aidar V. Fayzullin [1], Zulfiya R. Fayzullina [2] and Boris I. Kutepov [1]

[1] Institute of Petrochemistry and Catalysis, Ufa Federal Research Centre of the Russian Academy of Sciences (UFRC RAS), 450075 Ufa, Russia

[2] Department of Gas Chemistry and Modeling of Chemical-Technological Processes, Faculty of Technology, Ufa State Petroleum Technological University, 450064 Ufa, Russia

* Correspondence: maratradikovich@mail.ru

Abstract: The formation of intermediate phases during aging of the reaction gel composition $1.0Al_2O_3 \bullet 1.0P_2O_5 \bullet 1.5DPA \bullet 40H_2O$ and its subsequent crystallization into molecular sieves AlPO-11 and AlPO-41 was studied in this work. The initial gels and crystallization products were characterized by XRD; MAS NMR ^{27}Al and ^{31}P; scanning electron microscopy (SEM); transmission electron microscopy (TEM); and N_2-physical adsorption. It has been found that the nature of the aluminum source used to prepare the gel has a significant effect on the properties of the resulting intermediate phases. It is shown that by changing the chemical and phase composition of the intermediate aluminophosphate, it is possible to control the morphology and characteristics of the secondary porous structure of the AlPO-11 molecular sieve. The formation of the intermediate phases with a layered structure opens the possibility to synthesize high-phase purity AlPO-41 at the di-n-propylamine/Al_2O_3 ratio = 1.5. The formation mechanisms of AlPO-11 and AlPO-41 are proposed depending on the phase composition of the intermediate phases.

Keywords: zeolites; aluminophosphate molecular sieve; AlPO-11; AlPO-41; intermediate phases; micro-mesoporous materials; crystallization mechanism

1. Introduction

The achievements of the modern chemical industry are largely associated with the use of various molecular sieves [1,2]. Most of the zeolites used in industrial processes in their chemical composition are aluminosilicates. At the same time, molecular sieves based on aluminophosphates, AlPO-n, and their derivatives, MeAlPO-n and SAPO-n, are increasingly being used in catalysis and adsorption processes [3,4].

The first synthesis of AlPO-n molecular sieves was reported by Wilson et al. in 1982 [5]. Their porous crystal structures are formed from alternating AlO_4 and PO_4 tetrahedra linked via shared oxygen atoms. Like zeolites, such aluminophosphates are characterized by a wide variety of structures differing in pore size (AlPO-18 3.8Å × 3.8Å, AlPO-5 7.3Å × 7.3Å, VPI-5 12.7Å × 12.7Å) and channel dimensions (1D AlPO-11, 2D AlPO-57, 3D AlPO-34) [6]. AlPO-n molecular sieves, due to the presence of phosphorus atoms in their framework, provide a more effective isomorphic substitution of various elements compared to aluminosilicate molecular sieves. The introduction of Si or Mg atoms into the AlPO-n framework makes it possible to create promising acid catalysts on their basis [7], while the introduction of Co, Mn, and Fe metals makes it possible to create promising catalytic systems for oxidation [8]. In addition, AlPO-n molecular sieves are promising materials for gas separation [9], the creation of nanocarbon tubes [10], and optical systems [11].

Among the great variety of AlPO-n, molecular sieves AlPO-11 (structural type AEL) and AlPO-41 (structural type AFO) are of special interest due to the one-dimensional

channel structure with elliptical pores of 4.0Å × 6.5Å and 4.3Å × 7.0Å, which are comparable with the sizes of molecules of various practically important compounds. Based on the Si-containing molecular sieves SAPO-11 and SAPO-41, highly selective bifunctional catalysts have been developed for the hydroisomerization of C_{7+} n-paraffins [12,13]. Several studies have reported the high selectivity of SAPO-11 in the isomerization of n-butene to isobutylene [14] and the methylation of toluene to xylenes and naphthalene to dimethylnaphthalenes [15,16].

One of the distinguishing features of aluminophosphate molecular sieves compared to aluminosilicate ones is the formation of intermediate phases during their crystallization. It has been shown that during the crystallization of the AlPO-18 molecular sieve, amorphous aluminophosphate and the AlPO-5 molecular sieve are sequentially formed, and then the AlPO-5 is recrystallized to AlPO-18 [17]. It was found that various molecular sieves, such as AlPO-5, AlPO-22, AlPO-16, and SAPO-35, can be synthesized using one intermediate aluminophosphate with a layered structure only by changing the content of the template (hexamethyleneimine) in the reaction system [18]. In [19,20], during the crystallization of the AlPO-11 molecular sieve, the formation of an intermediate aluminophosphate with a layered structure, having 10-membered rings ordered only along the layer, was observed.

It is important to note that, in the works cited above, there is practically no information on the formation conditions and properties of various intermediate aluminophosphates, as well as on the influence of the nature of various intermediate phases on the morphology and porous structure of the AlPO-11 molecular sieve. The knowledge gained in the field of the formation of intermediate aluminophosphate phases and the influence on subsequent crystallization can become a powerful tool in the targeted regulation of the properties of AlPO-n molecular sieves.

The purpose of this work is to elucidate the effect of the chemical nature of the aluminum source used to prepare reaction gels and the conditions of their aging on the chemical and phase composition of intermediate aluminophosphates, as well as on the morphology and characteristics of the porous structure of AlPO-11 and AlPO-41 molecular sieves formed during subsequent crystallization.

2. Materials and Methods

2.1. Preparation of Initial Aluminophosphate Gels

The aluminophosphate gel composition for synthesis of the discussed molecular sieves was: $1.0Al_2O_3 \bullet 1.0P_2O_5 \bullet 1.5DPA \bullet 40H_2O$. Aluminum isopropoxide (iAl, 98%, Acros Organics, Noisy-le-Grand, France) and boehmite (SB, AlO(OH), 78% Al_2O_3, Sasol SB, Hamburg, Germany) were used as a source of aluminum for its preparation. Orthophosphoric acid (H_3PO_4, 85%, Reachim, Moscow, Russia) was used as a phosphorus source; di-n-propylamine (DPA, 99%, Acros Organics, Schwerte, Germany) was used as a template. The initial aluminophosphate gel was obtained as follows: 28 g of distilled water was added to 10.0 g of orthophosphoric acid, then 17.3 g of aluminumisopropoxide or 5.6 g of boehmite was added with vigorous stirring, then 6.6 g of di-n-propylamine was added. The resulting reaction mixture was vigorously stirred at 25 °C for 1 h until the formation of the homogeneous viscous gel. The aluminophosphate gel obtained by this method is labeled Gel-iAl using aluminum isopropoxide and Gel-SB using boehmite. Aluminophosphate gel Gel-iAl was white in color and had a viscosity of 30 cSt; sample Gel-SB had a similar color and viscosity of 50 cSt.

2.2. Preparation of Intermediate Aluminophosphate Phases

Intermediate aluminophosphates were prepared by keeping the initial Gel-iAl and Gel-SB gels in the temperature range from 25 to 140 °C for 24 h in stainless steel autoclaves equipped with PTFE liners. As a result of preliminary experiments, it was found that during the aging of the Gel-iAl gel in the range from 25 to 90 °C for 24 h, an amorphous phase is formed, and in the range from 90 to 140 °C for 24 h, a phase with a layered structure is formed. Aging of the Gel-SB gel in the range from 90 to 120 °C for 24 h leads to the

formation of hydroaluminophosphate $AlPO_4 \bullet 2H_2O$, and in the range from 120 to 140 °C for 24 h, a phase with a layered structure phase is formed. Table 1 shows the symbols of intermediate aluminophosphates and their aging conditions.

Table 1. Explanation of symbols aluminophosphates and their crystallization products.

Initial Gel	Gel Aging Temperature, °C	Intermediate Phase	Crystallization Products of Intermediate Phases
Gel-iAl	90	IF-iAl-90	AlPO-iAl-90
Gel-iAl	130	IF-iAl-130	AlPO-iAl-130
Gel-SB	90	IF-SB-90	AlPO-SB-90
Gel-SB	130	IF-SB-130	AlPO-SB-130

2.3. Crystallization of Aluminophosphate Molecular Sieves

Crystalline aluminophosphates were prepared from intermediate aluminophosphate phases by hydrothermal synthesis at 200 °C for 2 to 24 h. Preliminary experiments showed that cristobalite is formed during crystallization for more than 24 h. The resulting AlPO-n samples were washed with distilled water to a neutral pH, centrifuged at RCF = 2000 for 20 min, and dried at 100 °C for 48 h.

2.4. Characterization

X-ray diffraction (XRD) spectra of dried at 20 °C (72 h) gels, intermediate aluminophosphates, and samples of molecular sieves were collected by Bruker D8 Advance diffractometer using Cu Kα radiation. Scanning was carried out in the range of 2θ angles from 5 to 40° with a step of 1 deg/min. The phase analysis of the obtained X-ray patterns was carried out using the PDF2 database. X-ray images were processed using the TOPAS and Eva programs using the PDF2 database. The degree of crystallinity was estimated from the content of amorphous halo in the range from 20 to 30° 2θ using the TOPAS program.

^{31}P and ^{27}Al NMR were carried out on BrukerAvance-II 400 WB spectrometer using a 4 mm H/X MAS WVT probe with operating frequencies of 162.0 and 104.2 MHz, respectively, and a frequency VMU of 12 kHz. To obtain the MAS NMR spectra on ^{31}P nuclei, a single-pulse technique (90-degree pulse) was used with the following recording parameters: pulse duration, 2.1 μs; the number of repetitions, 32; and the time between repetitions, 120 s. The MAS NMR spectra on ^{27}Al nuclei were obtained using a 15-degree excitation pulse with a duration of 0.8 μs; 256 repetitions 256; and a time between repetitions of 0.5 s.

The morphology and crystal size of molecular sieves and intermediate phases were determined by field emission scanning electron microscopy (SEM). SEM images were recorded on Hitachi Regulus SU8220 scanning electron microscope. The images were taken in the mode of registration of secondary electrons at an accelerating voltage of 5 kV.

The microstructure of the samples was determined by transmission electron microscopy (TEM) on a Hitachi HT7700 electron microscope. The images were taken in the bright field mode at an accelerating voltage of 100 kV.

The BET surface area and the volume of micro- and mesopores were determined by nitrogen physisorption measurements using Quantachrome Nova 1200e sorptometer. Before the experiment, the samples were calcined at 600 °C for 5 h. The specific surface area was calculated using the multipoint BET method. The volume of micropores in the presence of mesopores was estimated by the t-Plot method. The pore size distribution was calculated using the BJH model (Barrett–Joyner–Halenda).

3. Results and Discussion

Controlling the morphology and crystal dispersion of molecular sieve crystals is one of the key problems that must be solved when creating materials with the desired properties for adsorption and catalysis [21].

Figure 1 shows the X-ray diffraction patterns of the dried initial gels and the intermediate aluminophosphates, and Table 2 shows their phase compositions and pH levels. It can

be seen that Gel-iAl is an amorphous phase, while Gel-SB is a mixture of di-n-propylamine phosphate (PDF №00-039-1892) and undissolved boehmite (PDF №00-001-1283). The introduction of the aging stage at 90 °C of the Gel-iAl does did not lead to a change in its phase composition. With a further increase in the aging temperature to 130 °C, a layered aluminophosphate material is formed, for which intense signals are observed on X-ray patterns at 6.5 and 8.0° 2θ. It was shown in [20] that the structure of this material is ordered only along the direction of the a-b plane and represents thin 2D plates connected by weak van der Waals forces and containing 10R rings. According to XRD data, the interplanar spacing (d), with characteristic of peaks at 6.2° (d = 14.0Å) and 8.0° (d = 11.0Å) observed in layered phases, is close to 6.5° (d~13.6Å) and 8.1° (d~10.9Å) in the theoretical (100) and (110) planes of the AEL (AlPO-11) structure, respectively. The results obtained indicate the presence of common structural fragments in the obtained layered aluminophosphates and AlPO-11 molecular sieve.
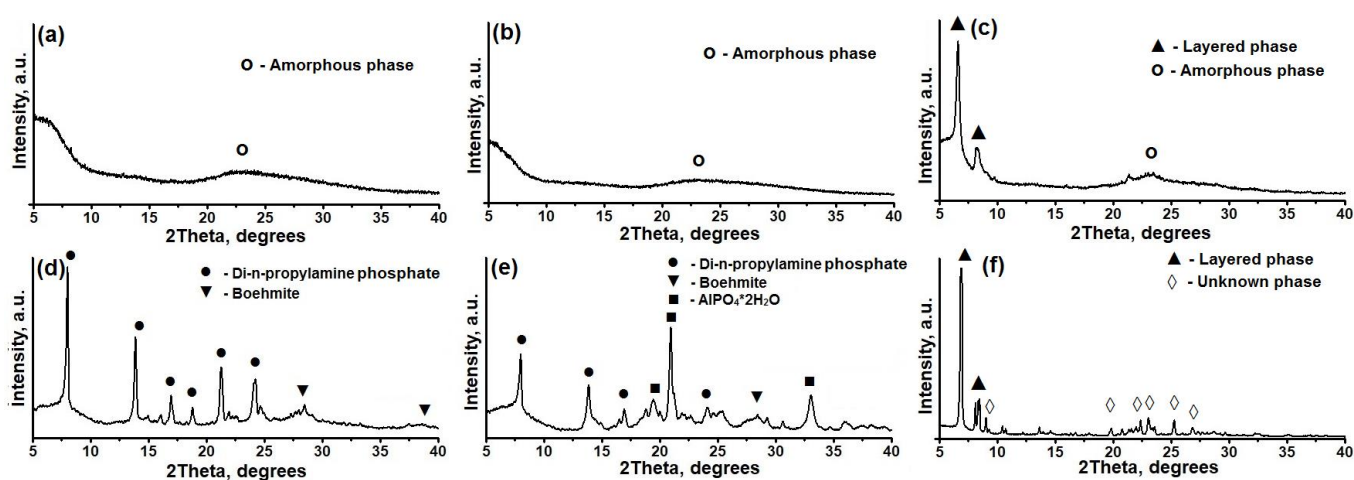

Figure 1. X-ray diffraction patterns of initial gels and intermediate phases: (**a**) Gel-iAl sample; (**b**) Sample IF-iAl-90; (**c**) Sample IF-iAl-130; (**d**) Gel-SB sample; (**e**) Sample IF-SB-90; (**f**) Sample IF-SB-130.

Table 2. Chemical and phase composition of initial gels and intermediate phases. Phase composition and pH of initial gels, intermediate phases of crystallization products.

Sample	Gel Aging Temperature, °C	pH	Phase Composition
Gel-iAl	-	7.6	AlPO$_4$ [1]
IF-iAl-90	90	8.1	AlPO$_4$
IF-iAl-130	130	8.5	Layered phase
Gel-SB	-	5.4	Ph.DPA + SB [2]
IF-SB-90	90	6.5	AlPO$_4$*2H$_2$O
IF-SB-130	130	8.2	Layered phase

[1]—Amorphous phase. [2]—Boehmit.

When Gel-SB is aged at 90 °C, di-n-propylamine phosphate reacts with undissolved boehmite to form hydroaluminophosphate AlPO$_4$•2H$_2$O (PDF №00-015-0311). The following temperature increase to 130 °C for the Gel-SB results in a layered aluminophosphate material. It was detected by the observation of the signals at 6.2° and 8.0° for X-ray patterns. Other weak signals at (13.4, 19.6, 20.5, 22.1, 22.8, 25.0, 26.6)° 2θ were attributed to the unidentified phases. It is important to note that the signal intensity in the X-ray diffraction patterns of the IF-SB-130 layered phase is significantly higher than that in the X-ray diffraction patterns of the IF-iAl-90 phase. The results obtained indicate a higher degree of crystallinity of the IF-SB-130 phase.

For a deeper understanding of the aging process of gels and the formation of intermediate phases, the MAS NMR spectra of [27]Al and ^{31}P were recorded, which are shown in Figure 2. It can be seen that in the [27]Al spectrum of the Gel-iAl gel, signals are observed at 42, 7, and −9 ppm. According to [19,20,22], the first signal is attributed to Al atoms with a tetrahedral oxygen environment [AlO$_4$] in amorphous aluminophosphate, a weak signal at 7 ppm is attributed to Al atoms with an octahedral oxygen environment [AlO$_6$] in an unreacted aluminum source, and a signal at −9 ppm is attributed to [AlO$_6$] in amorphous aluminophosphate. The ^{31}P spectrum of Gel-iAl shows signals at –6, –11, and –17 ppm. The signal at –6 ppm is attributed to phosphorus compounds in which P atoms are not bonded to Al atoms; apparently, this signal is due to the presence of unreacted orthophosphoric acid. The signals at –11 ppm and –17 ppm were assigned to aluminophosphates of the P(OAl)$_2$(H$_2$O)$_2$ and P(OAl)$_3$(H$_2$O) compositions, respectively [19,20,22]. As the Gel-iAl gel is aged at 90 °C, the MAS NMR [27]Al spectrum shows an increase in signal intensity at 42 ppm and a decrease in signal intensity at 7 ppm. The results obtained indicate a deeper interaction of boehmite with phosphoric acid at 90 °C with the formation of a material dominated by chemical bonds of the ≡Al-O-P≡ type.
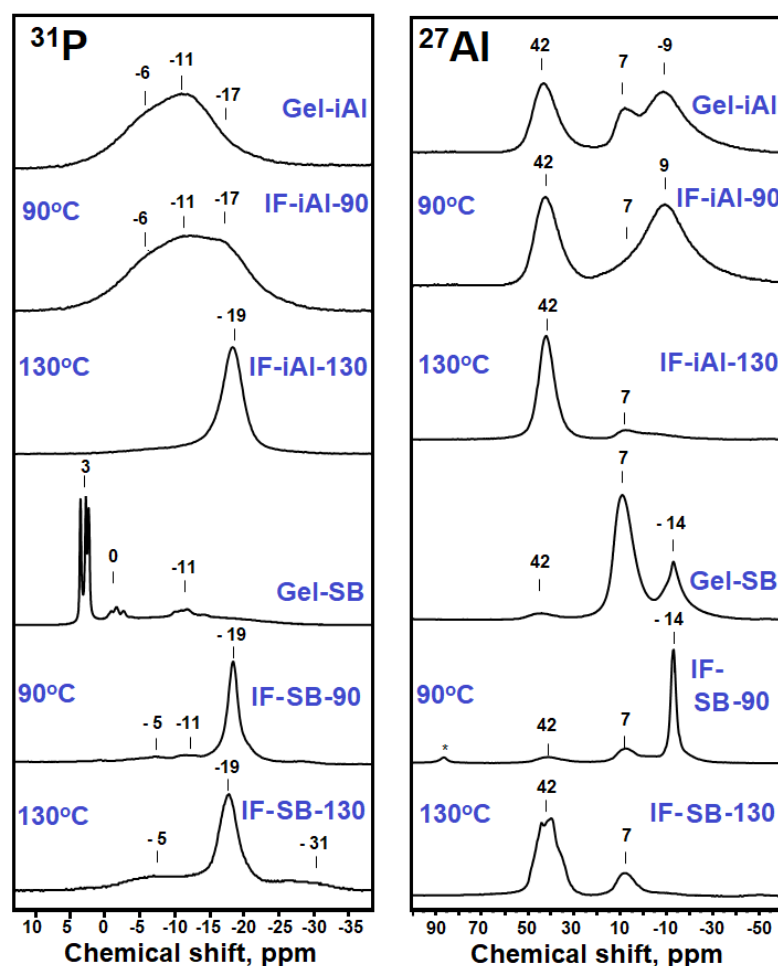

Figure 2. MAS NMR [27]Al and ^{31}P spectra of initial gels and intermediate phases.

In the MAS NMR spectrum of [27]Al of the layered phase (IF-iAl-130), the main signal is observed at 42 ppm, which is characteristic of [AlO$_4$], observed in molecular sieves, and in the ^{31}P spectrum, at –19 ppm, which is characteristic of [PO$_4$] in crystalline aluminophosphates. The obtained XRD and MAS NMR data of [27]Al and ^{31}P indicate that the intermediate phase, IF-iAl-130, is close in its structure to the structure of the AlPO-11 molecular sieve.

The MAS NMR spectrum of ^{27}Al Gel-SB shows a strong signal at 7 ppm and weaker signals at –14 and 42 ppm. Signals at 7 ppm and 14 ppm refer to aluminum atoms with an octahedral oxygen environment [AlO$_6$], which are characteristic of boehmite and amorphous aluminophosphate, respectively. The signal at 42 ppm is assigned to Al atoms with a tetrahedral oxygen environment [AlO$_4$] in amorphous aluminophosphates [19,20,22]. A group of signals at 3, 0, and –11 ppm are observed in the MAS NMR ^{31}P spectra of the Gel-SB sample. Based on XRD data (Figure 1), this signal corresponds to di-n-propylamine phosphate. The group of signals at 0 ppm corresponds to orthophosphoric acid. A broad signal at –11 ppm is the characteristic of aluminophosphates P(OAl)$_n$OH, where n varies from 1 to 4 [19,20,22]. Thus, the analysis of the MAS NMR ^{27}Al and ^{31}P spectra of the Gel-SB sample allows us to conclude that in gels prepared using boehmite, only a partial interaction of boehmite with orthophosphoric acid occurs with the formation of X-ray amorphous aluminophosphates, which are not detected by X-ray diffraction.

In the MAS NMR ^{27}Al spectrum of the intermediate phase IF-SB-90, signals are observed at –14 ppm associated with [AlO$_6$] in crystalline aluminophosphates and weak signals at 42 and 7 ppm, which, as noted above, are due to the presence of amorphous aluminophosphate and unreacted boehmite, respectively. In the MAS NMR ^{31}P spectra of the intermediate phase IF-SB-90, there is an intense signal at –19 ppm, which is attributed to [PO$_4$] in crystalline aluminophosphates. In addition, weak signals were recorded at –5 and –11 ppm. They are typical for aluminophosphates P(OAl)$_n$OH, where n varies from 1 to 4. Furthermore, a weak signal at 3 ppm was from di-n-propylamine phosphate. Comparing the intense signals at –11 ppm (^{27}Al) and –19 ppm (^{31}P) with the XPA data, we can assign them to the AlPO$_4$•(H$_2$O)$_2$ aluminophosphate phase.

Similar signals are observed in the MAS NMR ^{27}Al and ^{31}P spectra of the layered phase IF-SB-130, which also indicates the similarity of the structures of these phases for IF-iAl-130. However, in the ^{31}P spectrum for IF-SB-130, an additional weak signal is observed at −31 ppm, which indicates the presence of AlPO-n fragments of molecular sieves in its structure.

It should be noted that the pH values for the initial gels and intermediate phases are in good agreement with the MAS NMR ^{27}Al-^{31}P data. It can be seen that the more reactive aluminum isopropoxide reacts better with phosphoric acid already at the initial stages of gel preparation, forming ≡Al-O-P≡ bonds and forming aluminophosphate with a higher pH value than for the gel prepared using less reactive boehmite. For the intermediate phases IF-SB-130 and IF-iAl-130, the pH values are close because at 130 °C the aluminum source almost completely reacts with phosphoric acid to form aluminophosphate.

Figures 3 and 4 show SEM and TEM images of various intermediate phases. The IF-iAl-90 sample is a homogeneous material resembling a xerogel in structure and which is formed from spherical aggregates less than 10 nm in size. However, SEM images do not allow us to consider the structure of the primary particles that form the xerogel. The TEM image indicates that the IF-iAl-90 sample consists of spherical particles ranging in size from 5 to 10 nm. The IF-SB-90 sample consists of intergrowths ~5 μm in size, consisting of thin AlPO$_4$•2H$_2$O plates. The SEM images of samples IF-iAl-130 and IF-SB-130 show that they are characterized by a homogeneous structure. At the same time, there some areas are observed whose structure resembles a layered material. The TEM image of samples IF-iAl-130 and IF-SB-130 shows that their structure is formed from thin plates that look like crumpled papers in several layers. These thin plates have clear boundaries, the sizes of which are ~300 nm for the IF-iAl-130 sample and ~1000 nm for the IF-SB-130 sample. The difference in the plate sizes for samples IF-iAl-130 and IF-SB-130 is in good agreement with the X-ray diffraction data, from which it can be seen that for IF-SB-130, the signal intensities at 6.2° and 8.0° are higher than for IF-iAl-130.

To summarize, it is possible to obtain diverse intermediate phases by varying the sources of aluminum and aging temperatures of the initial gels. These collected phases differ significantly in chemical, phase composition, and morphology.
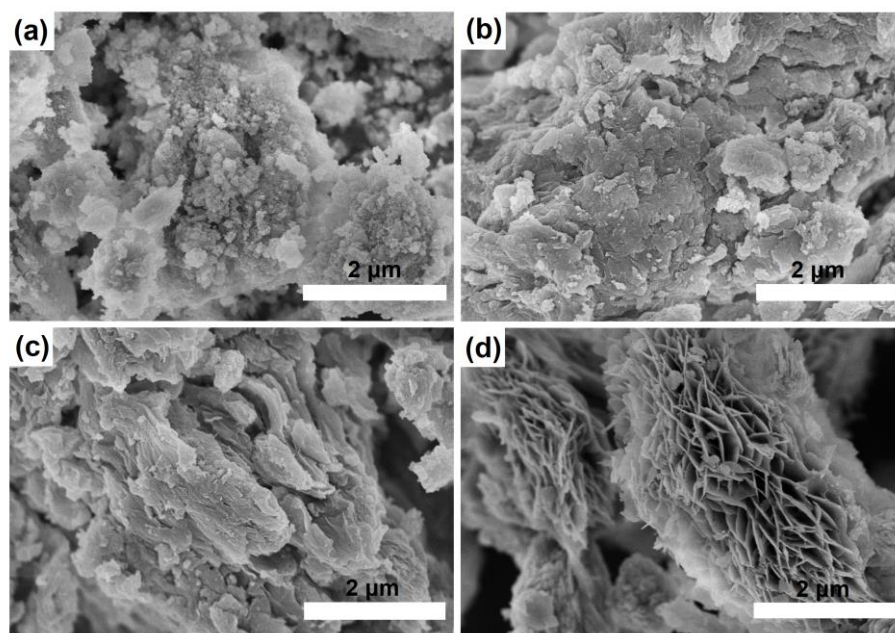
Figure 3. SEM images of intermediate phases: (**a**) Sample IF-iAl-90; (**b**) Sample IF-iAl-130; (**c**) Sample IF-SB-90; (**d**) Sample IF-SB-130.
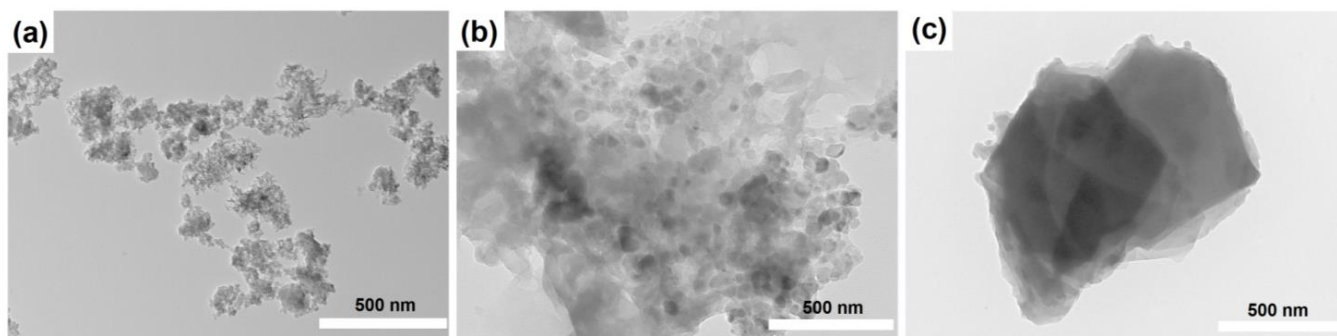

Figure 4. TEM images of intermediate phases: (**a**) Sample IF-iAl-90; (**b**) Sample IF-iAl-130; (**c**) Sample IF-SB-130.

Thus, the main reason for the formation of various intermediate phases from the initial gels of similar reactive composition is due to the complex effect of the reactivity of the aluminum source, the pH of the medium, and the aging temperatures. As noted above, Al isopropoxide, due to its higher reactivity compared to boehmite, almost completely reacts with phosphoric acid already at the initial stage of gel preparation. Due to this deeper interaction, higher supersaturations in the nuclei of the new phase arise with the formation of more dispersed amorphous or layered particles. Boehmite, due to its lower reactivity compared to aluminum isopropoxide, leads to the formation of non-porous $AlPO_4*2H_2O$ or a layered phase with larger particles.

Figure 5 shows the results of the crystallization of intermediate phases. It can be seen that during the crystallization of the IF-iAl-90, IF-iAl-130, and IF-SB-90 phases, the AlPO-11 molecular sieve begins to form already after 2 h, and after 4 h of crystallization, the main phase is AlPO-11. After 12 h of crystallization, the crystallinity of AlPO-11 is more than 90% for all samples. During the crystallization of the intermediate phase, IF-SB-130, the formation of AlPO-41 is observed after 2 h. After 12 h, this phase becomes the main one with a crystallinity of ~92%. It should also be noted that during the crystallization of AlPO-11 and AlPO-41 through the formation of intermediate phases, they are converted into molecular sieves without the formation of other intermediate phases.
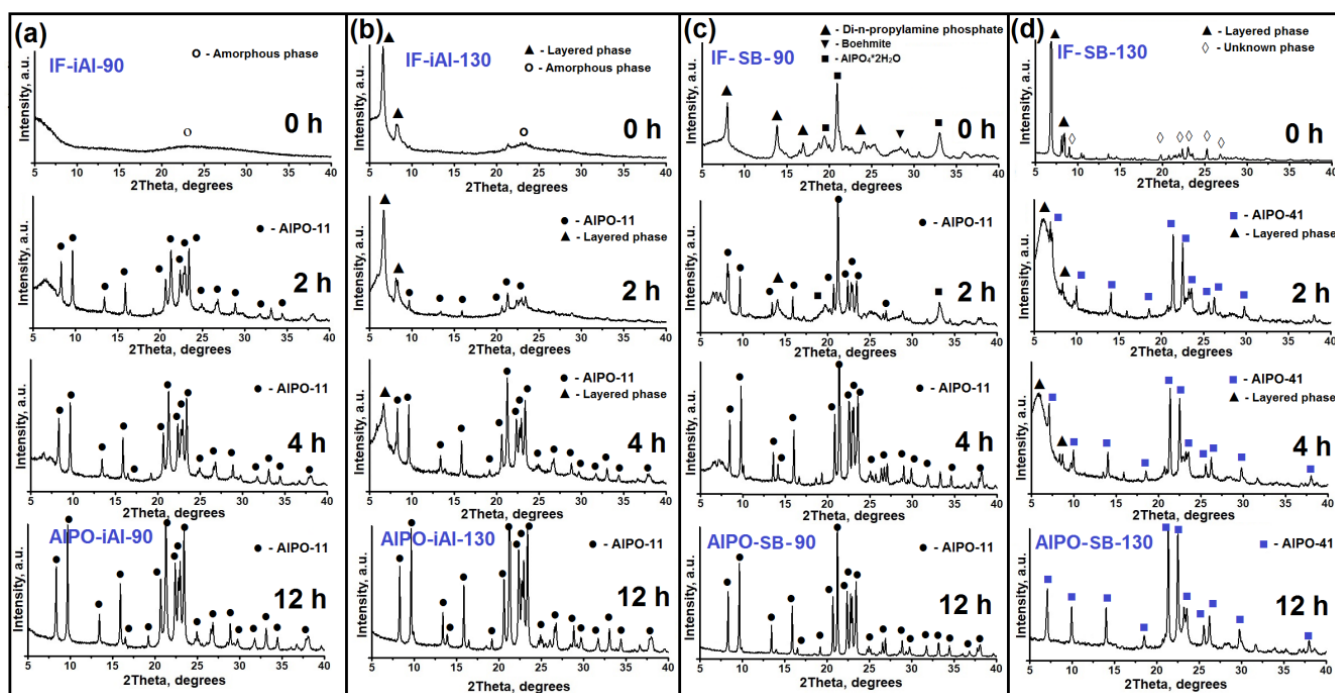
Figure 5. X-ray patterns of crystallization products of intermediate phases: (**a**) Crystallization of the intermediate phase IF-iAl-90; (**b**) Crystallization of the intermediate phase IF-iAl-130; (**c**) Crystallization of the intermediate phase IF-SB-90; (**d**) Crystallization of the intermediate phase IF-SB-90.

Thus, by preliminary forming an intermediate phase of different chemicals and phase compositions from aluminophosphate gel, it is possible to synthesize both the AlPO-11 molecular sieve and the AlPO-41 molecular sieve during further crystallization. Apparently, during the crystallization of the intermediate phase IF-iAl-130, due to the smaller size of the plates, it is easier to rearrange them into the AlPO-11 molecular sieve than into the AlPO-41 molecular sieve.

As noted above, the morphology and dispersion of molecular sieve crystals have a significant effect on their adsorption and catalytic properties. Figure 6 shows SEM images of samples of aluminophosphate molecular sieves synthesized using various intermediate phases. It can be seen that the IF-iAl-90 sample is a spherical aggregate ~5 μm in size, consisting of smaller crystals 200 × 1000 nm in size elongated in the form of thin needles. The crystals of the AlPO-11 sample obtained from the layered phase are aggregates of thin plates forming elongated cylinders from 2 to 3 μm in size. The crystals of the AlPO-11 sample obtained from the intermediate $AlPO_4 \bullet 2H_2O$ phases are regular prisms ~1 μm in size. The crystals of the AlPO-41 sample with a high degree of crystallinity are already octahedral prisms with a size of ~5μm.

Thus, it can be seen that by crystallizing the AlPO-11 molecular sieve through various intermediate phases, it is possible to control the morphology and dispersion of the crystals.

Figure 7 shows isotherms of the adsorption–desorption of nitrogen and the distribution of pores by size. Table 3 shows the characteristics of the porous structure of samples of molecular sieves AlPO-11 and AlPO-41. The type IV isotherms, which are typical for micro-mesoporous materials, were observed for AlPO-11 samples. These samples were prepared via the crystallization of intermediate phases based on Gel-iAl. Mesopores ranging in size from 2 to 25 nm are formed as a result of the incomplete coalescence of nanosized crystals. The AlPO-iAl-90 molecular sieve sample is characterized by a higher external specific surface and a larger mesopore volume than AlPO-iAl-130. It is associated with a smaller size of its primary crystals and their incomplete intergrowth. The type I isotherms of microporous materials are observed for samples of AlPO-11 and AlPO-41 molecular

sieves. These sieves, in turn, were obtained using intermediate aluminophosphate phases based on Gel-SB gel.
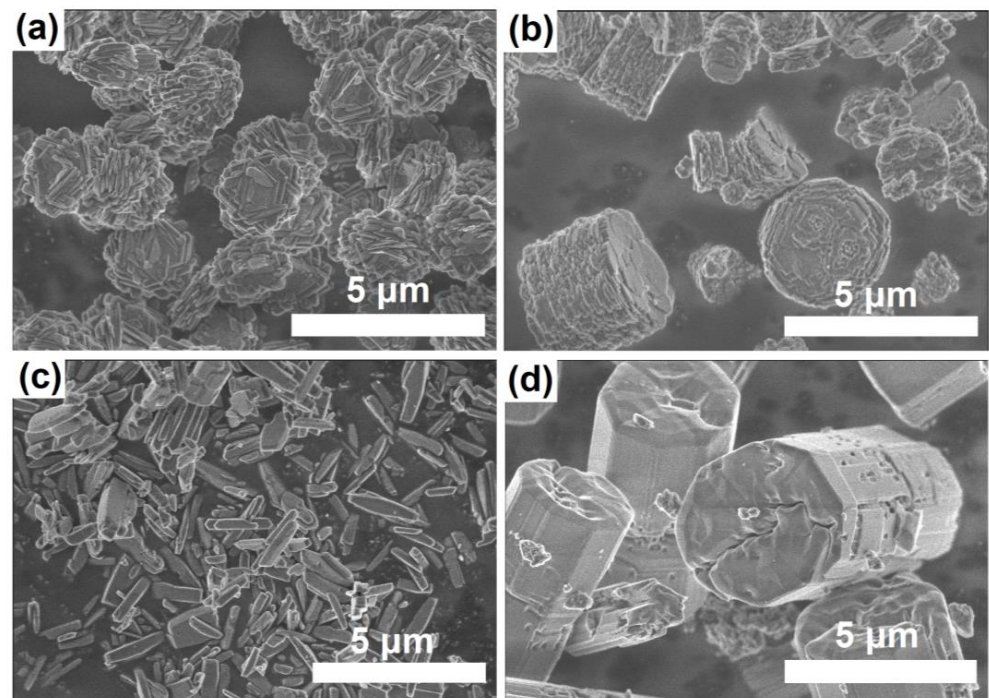

Figure 6. SEM images of molecular sieves: (**a**) Sample IF-iAl-90; (**b**) Sample IF-iAl-130; (**c**) Sample IF-SB-90; (**d**) Sample IF- SB-130.
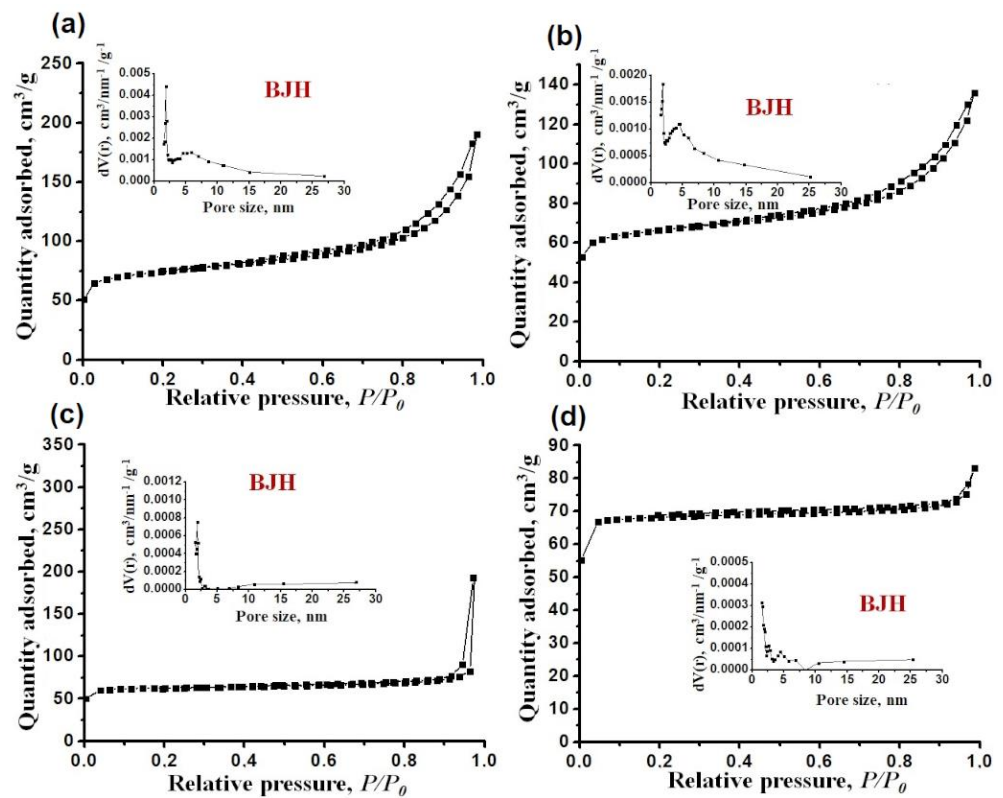

Figure 7. Nitrogen adsorption–desorption isotherms and pore size distribution of molecular sieves: (**a**) Sample IF-iAl-90; (**b**) Sample IF-iAl-130; (**c**) Sample IF-SB-90; (**d**) Sample IF-SB-130.
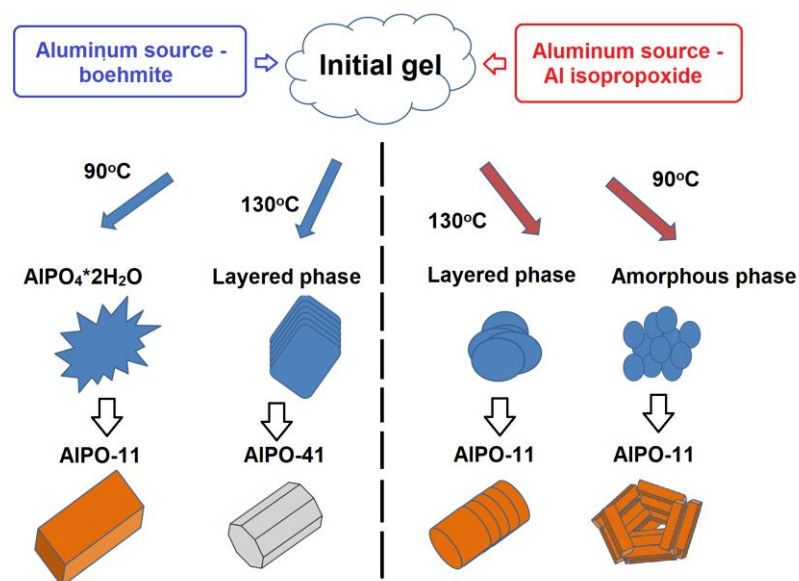
Table 3. Characteristics of the porous structure of molecular sieves.

Sample	S_{BET} [1], m^2/g	S_{EX} [2], m^2/g	V_{micro} [3], cm^3/g	V_{meso} [4], cm^3/g
AlPO-iAl-90	242	131	0.06	0.24
AlPO-iAl-130	215	85	0.07	0.15
AlPO-SB-90	196	54	0.07	0.07
AlPO-SB-130	211	51	0.08	0.05

[1]—specific surface according to BET. [2]—external specific surface. [3]—specific volume of micropores. [4]—specific volume of mesopores.

Thus, it follows from the above that, by changing the chemical and phase composition of the intermediate aluminophosphate phases, one can directionally control the morphology and characteristics of the porous structure of the AlPO-n molecular sieves crystallized from them.

The discussed results allow us to identify the following main stages in the formation of AlPO-11 and AlPO-41 molecular sieves from intermediate phases of various structures (Figure 8). The formation of an amorphous aluminophosphate gel occurs via an interaction between the aluminum isopropoxide added at the stage of mixing the initial substances at room temperature with orthophosphoric acid. At the same time, the formation of the mixture of di-n-propylamine phosphate and amorphous aluminophosphates occurs in the case of boehmite application. With further aging of the aluminophosphate gel at elevated temperatures, the formation of four different intermediate phases is possible.

Figure 8. The main stages of crystallization of molecular sieves from intermediate aluminophosphate phases.

From the gels prepared using aluminum isopropoxide, with further aging to 90 °C, an amorphous phase is formed, consisting of particles of aluminophosphate ~10 nm in size. At holding temperatures from 90 to 140 °C, a layered phase is formed, similar in structure to the AlPO-11 molecular sieve. It consists of thin layers ~500 nm thick, which are ordered along the layer plane.

From gels prepared using boehmite, with subsequent aging to 90 °C, hydroaluminophosphate is formed, which is composed of spherical aggregates from 2 to 3 μm in size, consisting of thin plates. At holding temperatures from 90 to 140 °C, a layered phase is formed, similar in structure to AlPO-11, which consists of thin layers ~1000 nm thick.

Depending on which of the listed phases undergoes further crystallization, it is possible to obtain spherical or cylindrical aggregates and regular-shaped crystals in the form of AlPO-11 molecular sieve prisms or crystals in the form of regular octagonal prisms AlPO-41 molecular sieve.

4. Conclusions

The formation of intermediate phases aged at 90–140 °C for the reaction gel (1.0Al$_2$O$_3$●1.0P$_2$O$_5$●1.5DPA●40H$_2$O) and its subsequent crystallization into molecular sieves AlPO-11 and AlPO-41 were studied.

The nature of the aluminum source (boehmite or aluminum isopropoxide) and the aging temperature of the initial gels (from 90 to 140 °C) have a significant effect on the properties of the formed intermediate phases. It was found that varying the intermediate aluminophosphate phase's chemical and phase composition before the crystallization at 200 °C enables the obtaining AlPO-11 or AlPO-41 molecular sieves with different crystal morphology and dispersion.

The aluminum isopropoxide-based gel was firstly aged at 90 °C. It resulted in the formation of the amorphous phase consisting of aluminophosphate particles from 5 to 10 nm in size. The subsequent crystallization of this intermediate phase led to the spherically aggregated particles of AlPO-11 5 μm in size. Gel aging at 130 °C led to the layered phase similar in structure to the AlPO-11. After its crystallization, elongated cylinders (2 to 3 μm) consisting of thin plates were formed.

The boehmite-based gel was heated to 90 °C for the formation of the spherical aggregates (5 μm). These structures were presented by thin hydroaluminophosphate AlPO$_4$●2H$_2$O plates. The following crystallization resulted in AlPO-11 with morphology composed of prisms (1 μm size). Boehmite-based gels pre-crystallization at 130 °C was applied for the formation of the layered phase with AlPO-11-like structure. The last one was represented by thin layers ~1000 nm in size. After the following crystallization AlPO-41 with octahedral prisms (5 μm) was collected.

Institutional Review Board Statement: Not applicable.

Informed Consent Statement: Not applicable.

Data Availability Statement: Not applicable.

Conflicts of Interest: The authors declare no conflict of interest.

References

1. Martínez, C.; Corma, A. Inorganic molecular sieves: Preparation, modification and industrial application in catalytic processes. *Coord. Chem. Rev.* **2011**, *255*, 1558–1580. [CrossRef]
2. Vermeiren, W.; Gilson, J.P. Impact of zeolites on the petroleum and petrochemical industry. *Top. Catal.* **2009**, *52*, 1131–1161. [CrossRef]
3. Potter, M.E. Down the microporous rabbit hole of silicoaluminophosphates: Recent developments on synthesis, characteri-zation, and catalytic applications. *ACS Catal.* **2020**, *10*, 9758–9789. [CrossRef]
4. Thomas, J.M.; Raja, R.; Sankar, G.; Bell, R.G. Molecular Sieve Catalysts for the Regioselective and Shape- Selective Oxyfunctional-ization of Alkanes in Air. *Accounts Chem. Res.* **2001**, *34*, 191–200. [CrossRef] [PubMed]
5. Wilson, S.T.; Lok, B.M.; Messina, C.A.; Cannan, T.R.; Flanigen, E.M. Aluminophosphate molecular sieves: A new class of microporous crystalline inorganic solids. *J. Am. Chem. Soc.* **1982**, *104*, 1146–1147. [CrossRef]
6. Baerlocher, C.; McCusker, L.B.; Olson, D.H. *Atlas of Zeolite Framework Types*, 6th ed.; Elsevier: Amsterdam, The Netherlands, 2007; pp. 1–404. [CrossRef]
7. Hartmann, M.; Elangovan, S. Catalysis with Microporous Aluminophosphates and Silicoaluminophosphates Containing Transi-tion Metals. *Adv. Nanoporous Mater.* **2010**, *1*, 237–312. [CrossRef]
8. Hartmarm, M.; Kevan, L. Transition-metal ions in aluminophosphate and silicoaluminophsphate molecular sieves: Location, interaction with adsorbates and catalytic properties. *Chem. Rev.* **1999**, *99*, 635. [CrossRef]
9. Zong, Z.; Elsaidi, S.K.; Thallapally, P.K.; Carreon, M.A. Highly Permeable AlPO-18 Membranes for N$_2$/CH$_4$ Separation. *Ind. Eng. Chem. Res.* **2017**, *56*, 4113–4118. [CrossRef]
10. Wang, N.; Tang, Z.K.; Li, G.D.; Chen, J.S. Single-walled 4 Å carbon nanotube arrays. *Nature* **2000**, *408*, 50–51. [CrossRef]

11. Hu, J.; Wang, D.; Guo, W.; Du, S.; Tang, Z.K. Reversible Control of the Orientation of Iodine Molecules inside the AlPO4-11 Crystals. *J. Phys. Chem. C* **2012**, *116*, 4423–4430. [CrossRef]

12. Yadav, R.; Sakthivel, A. Silicoaluminophosphate molecular sieves as potential catalysts for hydroisomerization of alkanes and alkenes. *Appl. Catal. A Gen.* **2014**, *481*, 143–160. [CrossRef]

13. Wang, W.; Liu, C.-J.; Wu, W. Bifunctional catalysts for the hydroisomerization of *n*-alkanes: The effects of metal–acid balance and textural structure. *Catal. Sci. Technol.* **2019**, *9*, 4162–4187. [CrossRef]

14. Mériaudeau, P.; Tuan, A.V.; Le Hung, N.; Szabo, G. Skeletal isomerisation of 1-butene on 10-member ring zeolites or on 10-member ring silico-alumino-phosphate microporous materials. *Catal. Lett.* **1997**, *47*, 71–72. [CrossRef]

15. Zhu, Z.; Chen, Q.; Xie, Z.; Yang, W.; Li, C. The roles of acidity and structure of zeolite for catalyzing toluene alkylation with methanol to xylene. *Microporous Mesoporous Mater.* **2006**, *88*, 16–21. [CrossRef]

16. Wang, X.; Guo, F.; Wei, X.; Liu, Z.; Zhang, W.; Guo, S.; Zhao, L. The catalytic performance of methylation of naphthalene with methanol over SAPO-11 zeolites synthesized with different Si content. *Korean J. Chem. Eng.* **2016**, *33*, 2034–2041. [CrossRef]

17. Huang, Y.; Demko, B.A.; Kirby, C.W. Investigation of the Evolution of Intermediate Phases of $AlPO_4$-18 Molecular Sieve Synthesis. *Chem. Mater.* **2003**, *15*, 2437–2444. [CrossRef]

18. Venkatathri, N.; Hegde, S.; Ramaswamy, V.; Sivasanker, S. Isolation and characterization of a novel lamellar-type aluminophosphate, $AlPO_4$-L, a common precursor for AlPO4 molecular sieves. *Microporous Mesoporous Mater.* **1998**, *23*, 277–285. [CrossRef]

19. Zhang, B.; Xu, J.; Fan, F.; Guo, Q.; Tong, X.; Yan, W.; Yu, J.; Deng, F.; Li, C.; Xu, R. Molecular engineering of microporous crystals: (III) The influence of water content on the crystallization of microporous aluminophosphate $AlPO_4$-11. *Microporous Mesoporous Mater.* **2012**, *147*, 212–221. [CrossRef]

20. Chen, B.; Huang, Y. Examining the self-assembly of microporous material $AlPO_4$-11 by dry-gel conversion. *J. Phys. Chem. C* **2007**, *111*, 15236–15243. [CrossRef]

21. Li, S.; Li, J.; Dong, M.; Fan, S.; Zhao, T.; Wang, J.; Fan, W. Strategies to control zeolite particle morphology. *Chem. Soc. Rev.* **2019**, *48*, 885–907. [CrossRef] [PubMed]

22. Xu, R.; Zhang, W.; Xu, J.; Tian, Z.; Deng, F.; Han, X.; Bao, X. Multinuclear Solid-State NMR Studies on the Formation Mechanism of Aluminophosphate Molecular Sieves in Ionic Liquids. *J. Phys. Chem. C* **2013**, *117*, 5848–5854. [CrossRef]